



ELSEVIER

Journal of Non-Crystalline Solids 305 (2002) 261–267

JOURNAL OF
NON-CRYSTALLINE SOLIDS

www.elsevier.com/locate/jnoncrysol

The effective permittivity of dense packings of glass beads, quartz sand and their mixtures immersed in different dielectric backgrounds

D.A. Robinson^{*}, S.P. Friedman

The Institute of Soil, Water and Environmental Sciences (ARO), The Volcani Center, Bet Dagan, Israel

Abstract

Dielectric methods, which measure the effective dielectric permittivity of granular materials, e.g., rocks, sediments and soils are often applied to estimate water or oil content. To test physically based models requires that the permittivity values of all phases are known. Measurements of the solid permittivity of glass spheres, quartz sand grains and their mixtures are made using an immersion method. The results obtained are tested against several classical models including the Maxwell Garnett, the symmetric effective medium approximation (SEMA) and the non-SEMA. The results demonstrate inadequate predictions between these models and the measured data. However, the Maxwell Garnett model comes close to predicting the effective permittivity of the media. Divergence between this model and the measurements is known to be due to interaction effects between grains that is not accounted for by a model based simply on the mixing of volumetric fractions of the components. With water as the background (contrast of 10 for glass) the Maxwell Garnett model overestimates the effective permittivity $\sim 5\%$ as the contrast reduces this error decreases. For contrasts < 4 the error for the permittivity estimate using the Maxwell Garnett formula was $< 3\%$. The modeling is simply used to demonstrate that the permittivity of the inclusions, for practical purposes, can be considered a linear function of the volumetric fraction times its respective permittivity. © 2002 Published by Elsevier Science B.V.

PACS: 77.22.-d; 77.22.Ch; 81.05.Rm

1. Introduction

Modeling of the effective permittivity of a granular material is of interest within geophysical, remote sensing and hydrological research [1–6].

Measurements are often used to estimate water and oil content within porous media. Direct calibration between measured permittivity and water/oil content is not always possible, nor always desirable. Therefore, the use of dielectric mixing models to estimate water/oil content from the measured permittivity of either saturated (2-phase, solid–liquid) or unsaturated (3-phase, solid–liquid–gas or solid–liquid–liquid) materials is often preferred [7–9]. In order to test models effectively it is important to know the permittivity of all the phases involved, the permittivity of the

^{*} Corresponding author. Present address: George E. Brown Jr Salinity Laboratory USDA-ARS, 450 W. Big Springs Road, Riverside, CA 92507, USA.

E-mail address: darobinson001@yahoo.co.uk (D.A. Robinson).

mineral matrix is often unknown and can contain minerals with different permittivity values. Values for quartz crystals cited from the literature lie between 4.3 and 4.7 [10] depending on crystal orientation and so values around this are often quoted for the permittivity of a mineral matrix of a quartz dominated granular material. Tables giving values of the permittivity of solid minerals are often estimates based on the use of mixing models to obtain the value of the solid permittivity from measurements of the effective permittivity of a repacked granular sample in air [11–13]. This requires the use of a theoretical model and pre-assumes the correctness of the model. Achieving accurate estimates of solid permittivity using repacked granular materials is not trivial as the permittivity of a 2-phase mixture depends on a number of factors [14].

2. Theoretical considerations

The method described in this work follows that described in [14] for determining the matrix permittivity of a granular solid by immersing it in a range of dielectric fluids. The immersion of a granular material in a dielectric fluid gives an effective permittivity somewhere between the permittivity of the background ϵ_0 and the permittivity of the granular inclusions ϵ_1 . By altering the permittivity of the immersion liquid the effective permittivity is also changed. To illustrate this we use the Maxwell Garnett [15] mixing model based on the Lord Rayleigh [16] formula. The Maxwell Garnett formula based simply on mixing the volumetric fractions of the components takes no account of the interaction effects between grains. Thus at porosities of 0.50–0.36 with high contrasts between the background and inclusions an error overestimating the effective permittivity by about 5% is expected when higher order multipole effects are not included [17]. However, this error becomes <3% for contrasts of <4, which is equivalent to <0.5 of a permittivity unit and acceptable for this work. Thus, with this in mind and the common use of the Maxwell Garnett model for describing a 2-phase mixture it is considered suitable for the present discussion.

$$\epsilon_{\text{eff}} = \epsilon_0 + 3f\epsilon_0 \left(\frac{\epsilon_1 - \epsilon_0}{\epsilon_1 + 2\epsilon_0 - f(\epsilon_1 - \epsilon_0)} \right). \quad (1)$$

The effective permittivity, ϵ_{eff} , of spheres in a background is described in terms of the background permittivity, ϵ_0 of volume fraction equal to the porosity, ϕ , and the permittivity of the solid inclusions, ϵ_1 of volume fraction, $f = 1 - \phi$. The model assumes that the solid spherical inclusions ‘see’ around themselves only the permittivity of the background. In reality in a densely packed granular mixture the background seen by the solid is some combination of solid and fluid and its respective permittivity. We therefore expect that the Maxwell Garnett model will be an upper bound where the background has a higher permittivity than the inclusion and a lower bound when this is reversed. The error between measured and predicted permittivity is therefore expected to increase as the contrast (ϵ_0/ϵ_1) between the two phases increases.

2.1. Porosity effects in different background permittivities

Fig. 1 illustrates the relationship between the effective permittivity, ϵ_{eff} , and the fluid permittivity, ϵ_0 , for a granular material with $\epsilon_1 = 5$, packed to three different porosity values. The 1:1 line is plotted on the diagram and demonstrates the convergence of all the predicted effective permittivity values to a single crossing point with the 1:1 line. The 1:1 line crossing point is physically significant, as this point is where the permittivity of the fluid is the same as the permittivity of the solid and the 2-phase mixture polarizes as a single unit. Above the crossing point the effective permittivity is lower than the permittivity of the immersion fluid and below the crossing point the effective permittivity is greater than that of the immersion background fluid.

The relationship between the effective permittivity of a 2-phase mixture and the bulk density to which it is packed is non-linear. Complicating this further is the particle shape [18] and particle size distribution [19], both of which affect the measured permittivity. Particle shape and orientation can strongly influence the effective permittivity, espe-

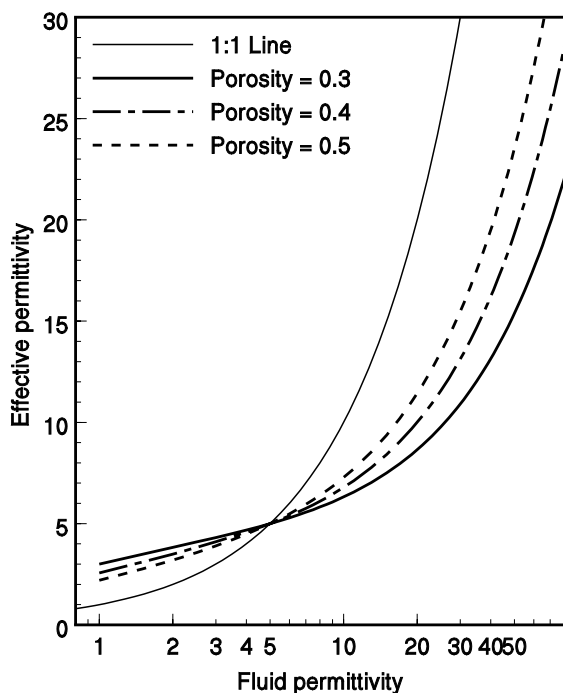


Fig. 1. Effective permittivity as a function of background permittivity modeled using the Maxwell Garnett formula. A solid with a permittivity of 5 is modeled with three porosity values demonstrating the porosity independence of the crossing point between the effective permittivity and the 1:1 line.

cially when the contrast between the fluid and inclusion is high (>5). The strength of the proposed method is that these effects do not influence the determination of the solid permittivity, unlike the estimates obtained from repacking powders at different bulk densities in air [11–13].

2.2. Mixtures of solids with different permittivities

Rocks and soils are nearly always a mixture of different minerals. The mixing model approach can be used to demonstrate the effective permittivity of a granular material with a mixture of inclusions with different permittivities. The effective permittivity of a mixture of inclusions is not that which is computed with the solid permittivity as a linear function of their volume fractions and their respective permittivities. This is demonstrated using a Maxwell Garnett based model for multiple inclusions with different permittivity values [8].

$$\varepsilon_{\text{eff}} = \varepsilon_0 + 3\varepsilon_0 \frac{\left[f_1 \left(\frac{\varepsilon_{1a} - \varepsilon_0}{\varepsilon_{1a} + 2\varepsilon_0} \right) + f_2 \left(\frac{\varepsilon_{1b} - \varepsilon_0}{\varepsilon_{1b} + 2\varepsilon_0} \right) \right]}{1 - \left[f_1 \left(\frac{\varepsilon_{1a} - \varepsilon_0}{\varepsilon_{1a} + 2\varepsilon_0} \right) + f_2 \left(\frac{\varepsilon_{1b} - \varepsilon_0}{\varepsilon_{1b} + 2\varepsilon_0} \right) \right]}, \quad (2)$$

where f_1 is the fraction of solid with permittivity ε_{1a} and f_2 is the volume fraction of solid with a permittivity ε_{1b} . This is illustrated in Fig. 2 for two solids, one with a permittivity of 5 and the other with increasing permittivity, 10, 15, 20 and 50. The corresponding effective permittivity in water ($\varepsilon_0 = 80$) is demonstrated in Fig. 2(a) according to Eq. (2). The overestimate using an arithmetic mean ε_1 for different contrasts ($\varepsilon_{1b}/\varepsilon_{1a}$) is given as a function of volume fraction of solid A mixed with solid B in water (Fig. 2(b)). A negligible effect for contrasts of 2 and lower is observed which means in the case of most soils, sediments and rocks the effective permittivity is almost that related to a matrix permittivity which is a linear combination of the volumetric fractions of the minerals and their respective permittivities. Even for a contrast of 10 between the inclusions the deviation of the linearly weighted ε_1 from the proper Maxwell Garnett prediction for the mixture is not very striking.

3. Materials and methods

3.1. Granular media

Two dielectric materials were chosen to test the method of immersing the granular media in different dielectric fluids: spherical glass beads made of soda lime silicate glass (Trime-IMKO, Germany) and acid washed quartz sand (Yerucham Crater, Negev desert, Israel). Their properties are listed in Table 1 with the particle densities determined using the standard excluded volume method.

3.2. Dielectric immersion fluids and packing

One of the difficulties in applying this type of method is finding fluids whose permittivities lie within a low permittivity range between 1 and 25. The fluids must not exhibit relaxation at the frequency of measurement and they must have a

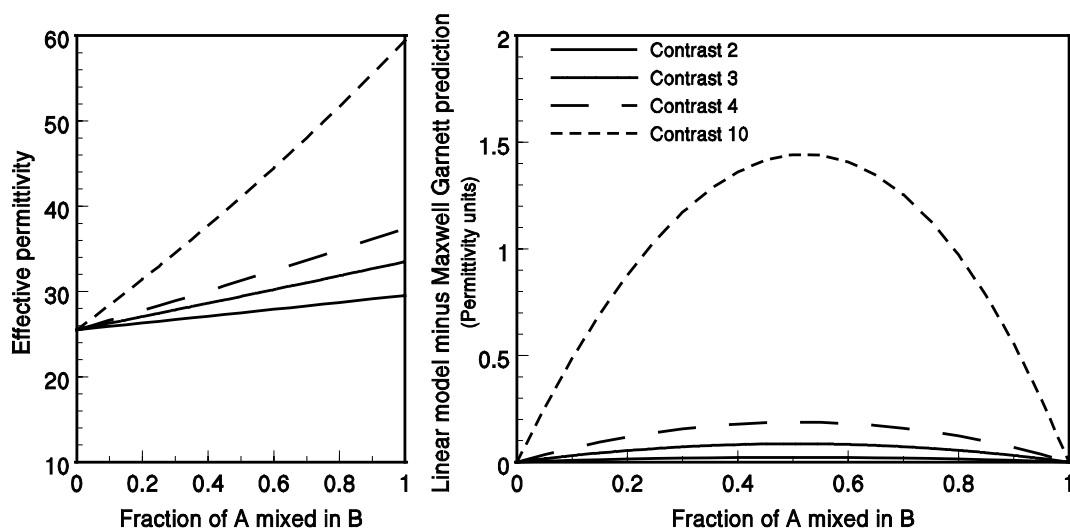


Fig. 2. Left: effective permittivity as a function of the fractions of two solid inclusions with permittivity contrasts of 2,3,4 and 10. Right: the linear fraction model minus the Maxwell Garnett prediction for the mixture.

Table 1
Experimental materials and physical properties

Material	Particle density (g cm^{-3})	Porosity	Composition
Glass spheres 500 μm	2.56	0.395	Soda lime silicate glass
Quartz sand 500 μm	2.65	0.382	Quartz

viscosity that allows the granular material to be mixed in the fluid, low viscosity fluids being the best. Air and water provide the limits of interest, with mixtures of water with acetone providing a permittivity range between ~ 20.8 and 78.6 and mixtures of methylene chloride and penetrating oil (WD-40[®]) providing a range between 2.3 and 8.8 . We found that alcohol is unsuitable as relaxation occurs in the MHz–GHz frequency range used here.

The first set of measurements had the granular samples carefully packed into a coaxial waveguide to a known porosity in air. The fraction of solid was then maintained for the subsequent measurements in other fluids to keep a constant porosity (Table 1). Sand grains were mixed into glass beads to give volume fraction ratios of 0.25 , 0.50 and 0.75 . The porosities of these mixtures were: 0.350 , 0.382 , 0.391 respectively.

3.3. Measurement of the effective permittivity

The effective permittivity was measured using a Tektronix (1502C) TDR cable tester. The time domain reflectometer (TDR) was connected to a computer, which was used to collect and analyze waveforms using software developed by Heimovaara and de Water [20]. The TDR was connected via a coaxial cable ($50\text{-}\Omega$ RG 58), 1.8 m long to a coaxial waveguide, constructed from steel, 200 mm long with an internal diameter of 26.5 mm and a 6 mm diameter inner electrode. The waveguide was calibrated for effective length using deionized water and air in a similar manner to Heimovaara [21]. This provides a measurement of permittivity accurate to ± 0.1 . Ten waveforms were collected using the TDR device and averaged to measure the effective permittivity of the mixture.

4. Results and discussion

Measurements of the grains were obtained using at least five dielectric solutions. A power function of the form $\epsilon_{\text{eff}} = a + b\epsilon_0^c$ was found to give a good empirical fit to the data points. This empirical curve was then used to find the intersection with the 1:1 line by equating ϵ_{eff} with ϵ_0 and solving iteratively for ϵ_0 to determine, ϵ_1 . Results for similar materials from the literature were found to be 6.75 [22] and 7.6 [14] for soda lime silicate glass and 4.3–4.7 for quartz crystals [10]. Our results were 7.6 for the glass, which is the same as the result for a similar glass presented in [14] and 4.7 for the quartz sand the same as in [10]. The close agreement with other results is very encouraging especially considering the probable difference in chemical composition between the glass used in these experiments [14], and the glass used by Von Hippel [22].

The effective permittivity measurements for glass beads are compared with three models in Fig. 3 using the obtained value of $\epsilon_1 = 7.6$ for the solid permittivity. Three classical models were conveniently combined into a single ‘heuristic’ model by Sihovla and Kong [23]

$$\epsilon_{\text{eff}} = \epsilon_0 + \left\{ \left[\frac{f(\epsilon_1 - \epsilon_0)[\epsilon_0 + a(\epsilon_{\text{eff}} - \epsilon_0)]}{3[\epsilon_0 + a(\epsilon_{\text{eff}} - \epsilon_0) + (\epsilon_1 - \epsilon_0)]} \right] \times \left[1 - \frac{f(\epsilon_1 - \epsilon_0)}{3[\epsilon_0 + a(\epsilon_{\text{eff}} - \epsilon_0) + (\epsilon_1 - \epsilon_0)]} \right]^{-1} \right\}. \tag{3}$$

The model presented for spheres has a single adjustable parameter a , confined between 0 and 1. A value of $a = 0$, results in the Maxwell Garnett [14] formula, $2/3$ gives the symmetric effective medium approximation (SEMA) [24,25], and $a = 1$ gives the coherent potential formula [26]. The equation results in an implicit formula for calculating the effective permittivity (ϵ_{eff}) for non-zero values of a . The other terms are as previously defined.

Presented alongside these models is the non-SEMA approximation proposed by Sen et al. [2] which can be considered the fractal limit for spheres, applicable for an infinitely broad particle size distribution

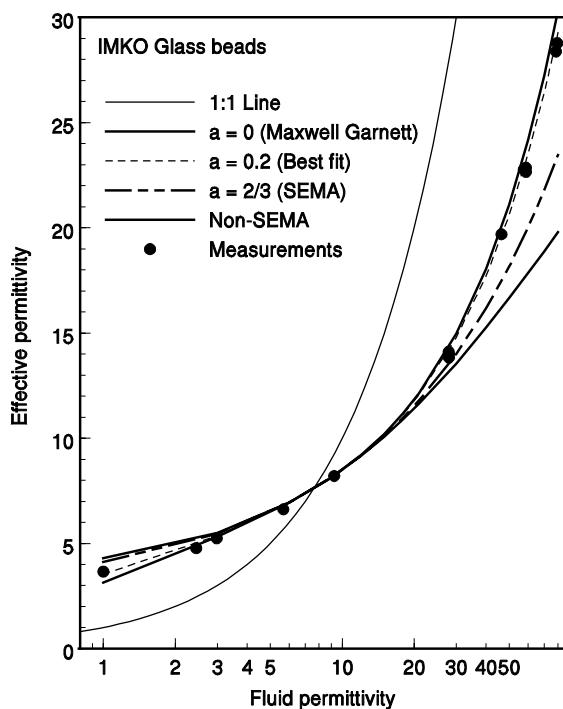


Fig. 3. The effective permittivity of IMKO glass beads ($\epsilon_1 = 7.6$) in different background permittivities measured with an absolute error in permittivity measurement of ± 0.1 . Data is modeled with the Maxwell Garnett (Eq. (1)), SEMA (Eq. (3), $a = 2/3$), and the non-SEMA (Eq. (4)) models. The ‘heuristic’ model (Eq. (3)) gave a best-fit to the data with the values of a set to 0.2.

$$\left[\frac{\epsilon_{\text{eff}} - \epsilon_1}{\epsilon_0 - \epsilon_1} \right] \left[\frac{\epsilon_0}{\epsilon_{\text{eff}}} \right]^{1/3} = \phi. \tag{4}$$

As discussed, for $\epsilon_0 > \epsilon_1$ the Maxwell Garnett model is expected to provide the upper bound and Sen et al. (Eq. (4)) the lower one. All the data fall between the expected upper and lower bound lying closest to the Maxwell Garnett prediction. As expected, the measured values are higher than the prediction of the model when air is the background. In the reverse case as the background permittivity rises above that of the solid so the experimental data points diverge from the Maxwell Garnett predictions. The result is that the Maxwell Garnett model over predicts the effective permittivity of glass spheres in water by $\sim 5\%$ as expected according to [17]. As the model and experimental material have the same geometry,

i.e. spheres, one can conclude that this over estimation of the effective permittivity is purely the result of the contact between grains. A fit was obtained between the heuristic model (Eq. (3)) and the data by adjusting the value of a to 0.2 (Fig. 3).

The data for the quartz sand grains are plotted in Fig. 4 along with the prediction of the Maxwell Garnett model. Again the effective permittivity in water is over estimated, in this case by $\sim 7\%$. This is likely to be a function of both the contact effect and the non-spherical shape of the grains. Both these effects act in the same direction reducing the effective permittivity.

Maxwell Garnett predictions (Eqs. (1) and (2)) are plotted with permittivity measurements taken for mixtures of sand and glass beads in Fig. 5. The porosities for these packings were: 0.350, 0.382 and 0.391 for the 0.25, 0.50 and 0.75 mixtures respectively. Results predicted with Eq. (2) clearly show

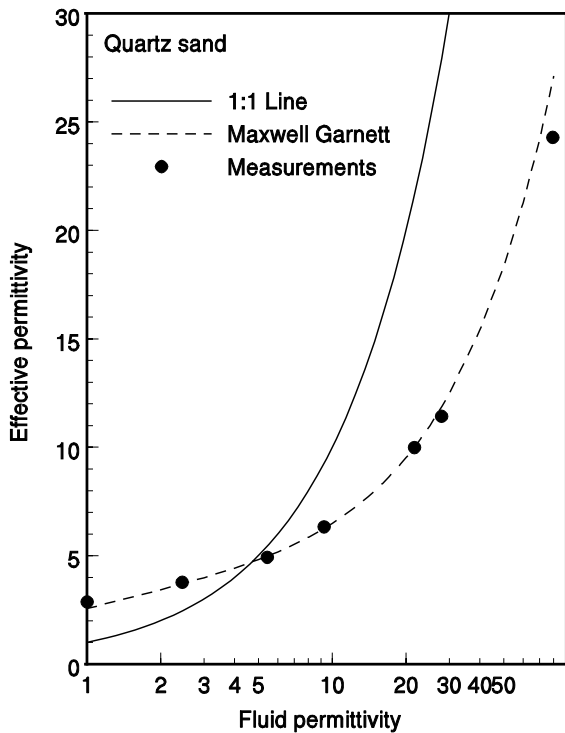


Fig. 4. The effective permittivity of quartz sand grains ($\epsilon_1 = 4.7$) in different background permittivities. Data is modeled with the Maxwell Garnett (Eq. (1)) formula. Absolute error in permittivity measurement ± 0.1 .

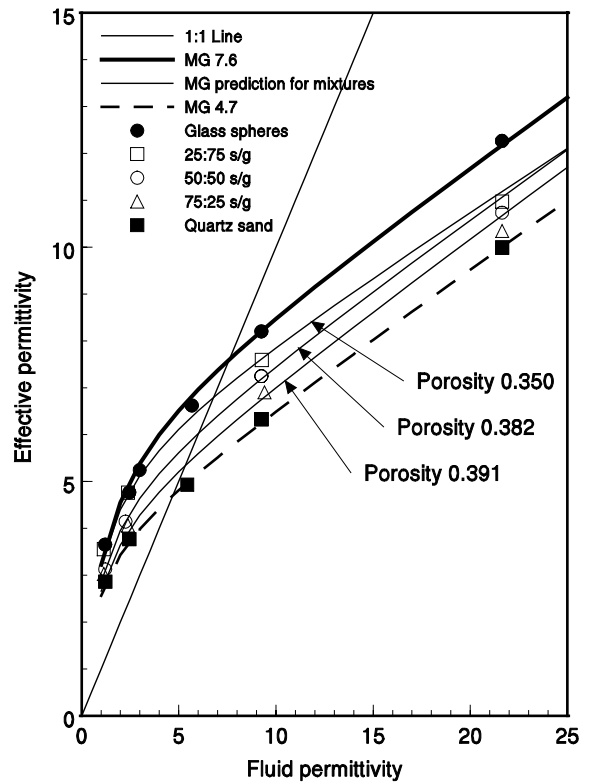


Fig. 5. Mixtures of quartz sand grains ($\epsilon_1 = 4.7$) mixed with IMKO glass beads ($\epsilon_1 = 7.6$). The thin solid lines represent the Maxwell Garnett (Eq. (2)) predictions for the three mixtures. Absolute error in permittivity measurement ± 0.1 .

the trend of permittivity decreasing as more sand is mixed into the glass. As the contrast (ϵ_0/ϵ_1) increases ($\epsilon_0 = 21$) so the effects of grain contact and particle shape become more noticeable, as a result the model and measurements diverge. The measurements suggest that at low contrast values the Maxwell Garnett model accurately predicts the effective permittivity of 2-phase granular media (Eq. (1)) and their mixtures (Eq. (2)).

5. Conclusions

Measurements of the solid permittivity of mixtures of glass beads and quartz sand are presented. The Maxwell Garnett mixing model is found to adequately predict the permittivity of the mixtures of quartz sand and glass beads when the solids are

in backgrounds with a contrast of <4 , as the error due to grain contact effects becomes small. The main conclusion being that for many practical purposes the arithmetic mean of the minerals solid permittivity can be used for modeling $\epsilon_{\text{eff}}(\phi)$. The determination of solid permittivity values using the immersion method enables the more thorough testing of dielectric mixing models, as the permittivity of all the phases can be determined. We use our data to demonstrate the inadequacies of applying mixing formulas based simply on the volumetric fractions of the components for contrasts up to 17. The importance of higher order multipole effects is demonstrated using a simple heuristic model accounting for interparticle contact effects.

Acknowledgements

This research was supported by research grant No. IS-2839-97, from BARD. The United States–Israel Binational Agricultural Research and Development Fund. Contribution from the Agricultural Research Organization, The Volcani Center, Bet Dagan, Israel, No. 606/01.

References

- [1] G.C. Topp, J.L. Davies, A.P. Annan, *Water Resources Res.* 16 (1980) 574.
- [2] P.N. Sen, C. Scala, M.H. Cohen, *Geophysics* 46 (5) (1981) 781.
- [3] M.T. Hallikainen, F.T. Ulaby, M.C. Dobson, M.A. El-Rayes, Lin-Kun Wu, *IEEE Trans. Geosci. Remote Sensing GE23* (1) (1985) 25.
- [4] C. Dirksen, S. Dasberg, *Soil Sci. Soc. Am. J.* 57 (1993) 660.
- [5] A.W. Kraszewski, in: A.W. Kraszewski (Ed.), *Microwave Aquametry Electromagnetic Wave Interaction with Water-Containing Materials*, IEEE, Piscataway, NJ, 1996.
- [6] R. Hilfer, *Phys. Rev. B* 44 (1) (1991) 60.
- [7] M.C. Dobson, F.T. Ulaby, M.T. Hallikainen, M.A. El-Rayes, *IEEE Trans. Geosci. Remote Sensing GE-23* (1) (1985) 35.
- [8] A. Shivola, *Electromagnetic Mixing Formulas and Applications*, *Electromagnetic Waves Series 47*, IEE, Michael Faraday House, Six Hills Way, Stevenage, UK, 1999.
- [9] S.P. Friedman, *Water Resources Res.* 34 (1998) 2949.
- [10] R.S. Carmichael, *Handbook of Physical Properties of Rocks*, CRC, Boca Raton, FL, 1982.
- [11] G.R. Olhoeft, in: Y.S. Touloukian, C.Y. Ho (Eds.), *Physical Properties of Rocks and Minerals*, McGraw-Hill/CINDAS Data Series on Material Properties, vol. II-2, McGraw-Hill, New York, 1981, p. 298.
- [12] S.O. Nelson, D.P. Lindroth, R.L. Blake, *Geophysics* 54 (10) (1989) 1344.
- [13] S.O. Nelson, T.-S. You, *J. Phys. D* 23 (1990) 346.
- [14] D.A. Robinson, S.P. Friedman, *J. Geophys. Res. B*, submitted for publication.
- [15] J.C. Maxwell-Garnett, *Philos. Trans. Royal Soc London A.* 203 (1904) 385.
- [16] L. Rayleigh, *Philos. Mag.* 34 (1892) 481.
- [17] A.G. Sangani, A. Acrivos, *Proc. Royal Soc. London A.* 386 (1983) 263.
- [18] S.B. Jones, S.P. Friedman, *Water Resources Res.* 36 (2000) 2821.
- [19] D.A. Robinson, S.P. Friedman, *Water Resources Res.* 37 (2001) 33.
- [20] T.J. Heimovaara, E. de Water, Report 41 Laboratory of Physical Geography and Soil Science, University of Amsterdam, Nieuwe Prinsengracht 130 1018 VZ, Amsterdam, 1993.
- [21] T.J. Heimovaara, PhD Thesis, Universiteit van Amsterdam, 1993.
- [22] A.R. von Hippel (Ed.), *Dielectrics Materials and Applications*, MIT, Cambridge, MA, 1954.
- [23] A. Sihvola, J.A. Kong, *IEEE Trans. Geosci. Remote Sensing* 26 (4) (1988) 20.
- [24] D.A.G. Bruggeman, *Ann. Phys.* 24 (1935) 636, in German.
- [25] D. Polder, J.H.V. van Santen, *Physica* 12 (5) (1946) 257.
- [26] L. Tsang, J.A. Kong, R.T. Shin, *Theory of Microwave Remote Sensing*, John Wiley, New York, 1985.